Performance assessment of a photovoltaic/thermal-powered absorption chiller for a restaurant

Nima Monghasemi [a,*], Stavros Vouros [b], Konstantinos Kyprianidis [c], Amir Vadiee [d]

[a,c] *School of Business, Society, and Engineering, Division of Sustainable Energy Systems, Mälardalen University, Sweden*

[b] *Academy for Innovation, Design and Technology, Department of Product Realization, Mälardalen University, Sweden*

[d] *School of Business, Society, and Engineering, Division of Sustainable Environment and Construction, Mälardalen University, Sweden*

nima.monghasemi@mdu.se

Abstract

In recent years the demand for cooling in buildings has grown steadily due to factors such as climate change and increased use of technology in Sweden. The increase of cooling demand occurs mainly during peak demand periods, where there is limited cooling capacity combined with limited distribution capacity in the district cooling network. Sweden has experienced considerable growth in the solar energy market in recent years, though its utilization has been mostly limited to power generation. To fulfill the cooling demand increase, solar driven cooling is a viable solution alternative to traditional cooling methods. The use of solar cooling is still in its early stages in Sweden. The aim of this work is to design a simulation model of a solar absorption cooling system for a full-service restaurant prototype building. The system layout consists of photovoltaic/thermal collector, storage tank, single-effect absorption chiller, auxiliary heater, and cooling tower. The results revealed the system ability to meet the cooling load while delivering sufficient hot water for the establishment. Higher solar fraction confirmed that using photovoltaic/thermal collector is more competitive than solar thermal collectors based on restaurant operational activities. A levelized cost of cooling of 0.164 €/kWh indicated the system cost-effectiveness in comparison to similar setups in other favorable European locations for solar energy utilization.

Keyword: Solar cooling, Absorption cooling, Photovoltaic/thermal collector, TRNSYS

Nomenclature

Symbol	Description	Unit
A	Area	m^2
C	Heat capacity	kJ kg^{-1} K^{-1}
c_p	Specific heat capacity	$Jkg^{-1}K^{-1}$
C_{elec}	Electricity price	€ kWh^{-1}
C_I	Capital investment cost	€
C_{om}	Operating and maintenance cost	€
f	Fraction of rated capacity	–
G	Solar radiation	W m^{-2}
h	Specific enthalpy	kJ kg^{-1}
k	Thermal conductivity	W m^{-1} K^{-1}
L	Distance	m
$\dot{m}$	Mass flow rate	kg s^{-1}
N	Lifespan	year
P	Power	kW
$\dot{Q}$	Heat transfer rate	kW
r	Discount rate	–
T	Temperature	℃
t	Time	s
U	Heat loss coefficient	W m^{-2} K
τ	Transmittance	–
$\dot{W}$	Work	kW
η	Efficiency	–
Subscripts		
aux	Auxiliary	
bot	bottom	
c	Cooling	
chw	Chilled water	
cw	Cooling water	
el	Electrical	
edg	edge	
hw	Hot water	
j	jth node	
out	Outlet	
tank	Storage tank	
th	Thermal	
top	top	
t	Thermal	

Abbreviations		
ANN	Artificial neural network	
COP	Coefficient of performance	
LCOC	Levelized cost of cooling	€ kWh^{-1}
NPC	Net present cost	€
PV/T	Photovoltaic thermal	
SF	Solar fraction	

1. Introduction

The building sector within both the EU and Sweden accounts for about 40% of total energy use (Liu, Rohdin, & Moshfegh, 2015). Space cooling is the fastest-growing use of energy in buildings, both in hot and humid emerging economies where incomes are rising, and in the advanced industrialized economies where consumer expectations of thermal comfort are still growing (IEA, 2018). In Sweden, about 14% of the service sector buildings apply space cooling and about half of these cooling demands were met by district cooling deliveries (Werner, 2017). There are still several potential barriers to installing district cooling in Sweden, such as high upfront costs, a lack of awareness about district cooling systems, and existing infrastructure and property technology limitations. Additionally, legal barriers may also pose challenges for implementing district cooling on a large scale (Palm & Gustafsson, 2018). Cooling demand is expected to continue in the foreseeable future, putting pressure on the country's energy infrastructure. Therefore, finding sustainable and efficient alternative cooling solutions for buildings in Sweden is of importance.

Solar cooling systems offer a sustainable and eco-friendly alternative for air conditioning purposes, as they do not rely on electricity generated from fossil fuels but rather utilize solar energy (Palomba et al., 2017).

A solar absorption cooling system is a type of air conditioning system that uses solar energy to power its cooling cycle. There are several research efforts being conducted on the use of solar absorption chiller systems for cooling applications. Lubis et al. (2016) evaluated the performance of a single-double-effect absorption chiller in tropical Asia regions. During daytime hours, the energy saving could be up to 48% compared with an equivalent vapor compression chiller. Abdullah, Saman, Whaley, and Belusko (2016) investigated the potential of operating a solar-driven absorption chiller for a typical Australian home. The modelling and dynamic simulation of the integrated system

were performed using TRNSYS software and GenOpt ("GenOpt," 2009) was used for optimal sizing of the components. Although the system exhibited a 75% reduction in critical peak power demand, the payback period of the investment was not justified.

Integration of solar absorption systems with other technologies such as energy storage and heat pumps increase the flexibility of the system and making it more practical for use in different applications. Borhani, Kasaeian, Pourmoghadam, and Omid (2023) analyzed the dynamic performance of a photovoltaic/thermal (PV/T) system coupled with an auxiliary heater and an absorption chiller, enabling the generation of electricity, heating, and cooling simultaneously. An artificial neural network (ANN) forecasting model was also developed to predict the system's performance under various climate conditions. Yue et al. (2023) proposed a solar tri-generation supply system that combines a PV/T collector, a heat pump, and an absorption chiller into a single integrated unit. The findings indicated that the system satisfied the load demand of a building in China, achieving an energy efficiency of 32.98% and an exergy efficiency of 17.62%. Moreover, the payback period was estimated to be 7.77 years, which was reasonable in comparison with other conventional systems.

The use of solar absorption cooling in Sweden is currently limited. With the anticipation of increasingly warmer summers in Sweden, the present study aims to assess the feasibility of a solar-assisted chiller powered by PV/T for the purpose of solar cooling. As an added benefit, this system also provides hot water delivery. The motivation behind this dual-purpose system for the restaurant application is threefold. Firstly, it allows the establishment to meet its high temperature hot water needs for sanitization and dishwashing. While district heating is a convenient source of hot water, its supply temperatures cannot meet these specific requirements. Secondly, by utilizing a PV/T system, solar energy is harnessed efficiently for both electricity and heat production, enabling the restaurant to maximize solar energy utilization. Lastly, the system configuration enables heat recovery through a heat exchanger that captures excess heat from the chiller outlet flow to preheat water. Without this heat recovery, the excess heat would otherwise be wasted in the cooling tower discharge.

2. System overview

The schematic of the proposed energy system is shown in Fig. 1. The system comprises a PV/T collector, heat storage tank, auxiliary fluid heater, absorption chiller (AC), and cooling tower, and heat exchanger. The heat storage tank is also equipped with an auxiliary heater in case the solar hot water generation is not sufficient. The AC is a lithium bromide/water single effect-absorption chiller. The PV/T panels produce heat and electricity simultaneously. The thermal storage tank stores hot water from the PVT for hot water usage (state 6) based on the hot water demand profile. When there is a cooling demand, the hot water is transferred to the absorption chiller (state 12). The generated electricity will first be dedicated to powering the chiller and the pumps. The surplus power is then either used for charging the storage tank via an electric coil or in case the tank demand is fully met, it is used in the auxiliary fluid heater to achieve the desired hot water inlet temperature for the chiller (state 12). The energy system in this setup operates without the requirement for battery storage, aiming to maximize cost-effectiveness. The panels and storage unit are appropriately sized to meet a portion of the restaurant's energy demand independently from the heating network and electricity grid. However, the building remains connected to the electricity grid to ensure a continuous supply of energy in case of any shortage. The primary function of the diverter is to control the distribution of hot water flow, effectively directing it to either the storage tank (state 10) or the chiller (state 11). When pump 1 is running, the controller prioritizes supplying water as heat source for the chiller based on the cooling schedule demand. The surplus heat is used for charging the storage tank. The tempering valve splits the input cold water (state 1) between the tee piece 1 and the heat exchanger (state 3). The heat exchanger is used to preheat the cold water before it enters the storage tank (state 4). The source side fluid stream carries the water release from the absorption chiller (state 16) acting as the heat source for the heat exchanger. After cooling down through the heat exchanger (state 17), pump 2 sends the flow back to the tee piece 2 in which it is being mixed with the chiller cooling water (state 15) before delivering it to the cooling tower (state 19). This approach is considered as heat recovery, where the excess heat from the chiller source side is utilized before it is ultimately rejected to the cooling tower. The chilled water is pumped from the absorption chiller unit into a distribution system (state 13). The chilled water carries heat away from the medium and delivers it back to the absorption chiller for the cycle to repeat (state 14).

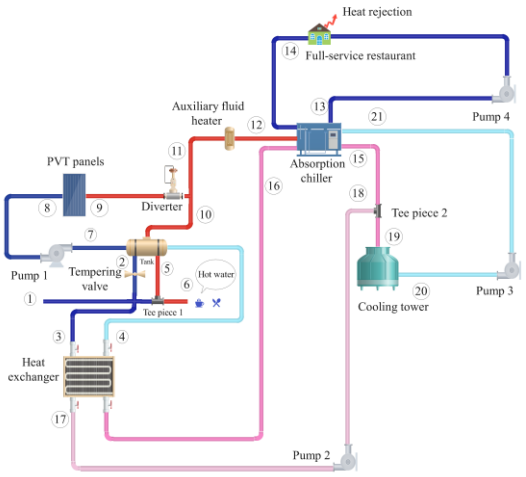

Figure 1. Schematic diagram of the proposed cooling system.

The simulations are performed using TRNSYS software, known for its extensive capabilities in transient modeling of renewable energy systems. All components adopted in this system were provided by the components library. The specification of each component is declared in Tab. 1

Table 1. The components and parameters of the system.

Parameter	Value
PV/T panel	
Collector area	150 m^2
Collector efficiency factor	0.7
Collector plate absorptance	0.9
Collector plate emittance	0.9
Bottom and edge losses coefficient	20 kJ/hm^{2}K
Collector slope	40°
Temperature coefficient of PV cell	-0.0003 1/K
Cell efficiency at reference condition	0.2
Packing factor	0.5
Thermal storage tank	
Tank volume	3 m^3
Tank height	1 m
Top, edge, and bottom loss coefficient	2.5 kJ/hm^{2}K
Absorption chiller	
Rated capacity	80 kW
Rated Coefficient of performance	0.53
Auxiliary electrical power	5 kW

In this work the chilled water is circulated within a full-service restaurant to absorb heat from its desired space. Given the lack of reliable and consistent experimental data from a commercial building with proposed energy system, the authors made the decision to employ a prototype building model as an alternative. The building model used in this study is based on the full-service restaurant model developed by the U.S. Department of Energy (Deru et al., 2011). The building is divided into three thermal zones: kitchen, dining space, and an unconditioned attic. Modifications have been made to the model to represent the building in Sweden (Boverket, 2019). The geometrical and thermal properties of the building are presented in Tab. 2 and Tab. 3, respectively.

Table 2: Geometrical parameters of building.

Parameter	Value	Unit
Area	511	m^2
Floor	Single floor plus attic	-
Floor to ceiling height	3.048	m
South window-wall ratio	28	%
East window-wall ratio	20.22	%
North window-wall ratio	0	%
West window-wall ratio	20.22	%

Table 3. Thermal specifications of model.

Parameter	Value	Unit
Exterior wall	0.29	W/m^2K
Roof	0.12	W/m^2K
Window	2.04	W/m^2K
Interior partition	6.3	W/m^2K

Internal heat loads consist of plug and process loads (157 W/m^2) and lights (20.4 W/m^2). The number of people per floor area is 0.8. Fig. 2 shows the occupancy hourly schedule for weekdays that is used to control the operation of absorption chiller as well.

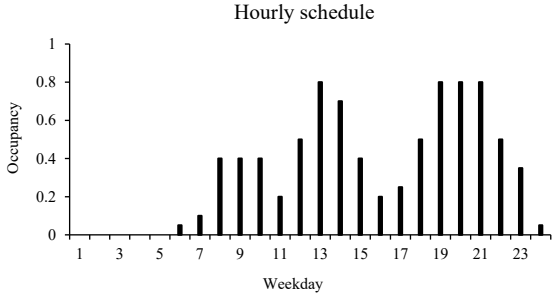

Figure 2. Building occupancy schedules on a weekday.

Fig. 3 gives information about the hourly hot water demand profile of the restaurant based on summer design schedule (Fuentes, Arce, & Salom, 2018; Murakawa, Nishina, Takata, & Tanaka, 2005).

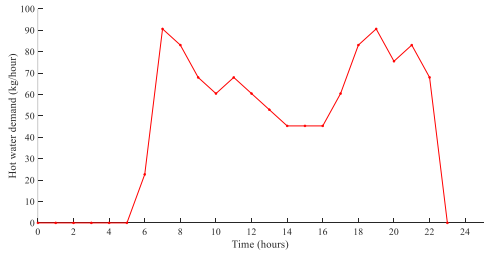

Figure 3. Building hot water draw-off profile.

The primary purpose of the absorption chiller is to meet the cooling requirements of the building. It does so by absorbing heat from the building's cooling load, transferring it to the refrigerant, and ultimately rejecting the heat to the environment through the condenser. The restaurant is divided into two thermal zones, one is the kitchen and the other is the dining area. The cooling setpoint for the dining area is 24°C, while it is 26°C for the kitchen. The cooling load of the restaurant model is shown in Fig. 4. The maximum cooling load is 38.8 kW.

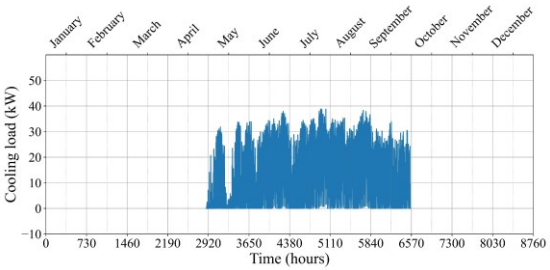

Figure 4. Restaurant hourly cooling load.

3. Modeling

The thermodynamic modeling of the system is divided into multiple subsystems, which include the PV/T panels, heat storage tank, absorption chiller, and the auxiliary components.

3.1. Thermodynamic analysis

The energy assessment aims to analyze the energy conversion quantities, considering the transient behavior of each component. The calculation involves determining the mass and energy balance equations for each component in the system as below (Behzadi & Arabkoohsar, 2020):

$$\sum \dot{m}_{in} = \sum \dot{m}_{out} \quad (1)$$

$$\dot{Q} - \dot{W} = \sum \dot{m}_{out} h_{out} - \sum \dot{m}_{in} h_{in} \quad (2)$$

By applying mass balance and energy balance principles to each component, one can assess its performance.

3.1.1. PVT panels

Th power output from the PV/T panels is directed toward different components based on their electricity demands. The generated electricity is primarily utilized to power the absorption chiller and its associated components such as solution and refrigerant pumps. The surplus power will be used to charge the thermal storage tank via an electrical coil and operating the pumps. If the storage tank is fully charged, the excess power is then utilized by the auxiliary fluid heater.

The electrical and thermal efficiency of the PV/T are as follows:

$$\eta_{el} = \frac{P_{el}}{\tau G A_p} \quad (3)$$

$$\eta_{th} = \frac{Q_u}{\tau G A_p} \quad (4)$$

in which:

$$Q_u = \dot{m}_8 c_p (T_9 - T_8) \quad (5)$$

where η_{el} is the electrical efficiency, G is total incident solar radiation on the collector surface, P is electric power output, τ is the glass cover plate transmittance, $\dot{m}_8$ is water mass flow rate to the panel at state 8, T_9 and T_8 are the outlet and inlet temperature at states 9 and 8, respectively.

The total efficiency of the PV/T panels is determined by adding the electrical efficiency and thermal efficiency as:

$$\eta_{PVT} = \eta_{el} + \eta_{th} \quad (6)$$

3.1.2. Thermal storage tank

The component represents a cylindrical constant volume liquid storage tank with a vertical orientation. It can interact with up to two flow streams and incur thermal losses through the top, bottom, and edges. The tank is divided into temperature nodes to model temperature stratification and each node is governed by the tank energy balance as a function of time (Khan, Badar, Talha, Khan, & Butt, 2018). Through trial-and-error testing of models with varying numbers of nodes, 6 nodes were found to provide the balance between accuracy and computational efficiency. Using more than 6 nodes provided minimal improvements in outlet temperature accuracy while increasing simulation runtimes. The differential equation for the tank nodes can be written as:

$$\frac{dT_{tank,j}}{dt} = \frac{Q_{in,tank,j} - Q_{out,tank,j}}{C_{tank,j}} \quad (7)$$

where $T_{tank,j}$ is temperature of the tank node j, $Q_{in,tank,j}$ and $Q_{out,tank,j}$ is the heat input and output for node j and can be expanded as follows:

$$Q_{in,tank,j} = Q_{aux,t} + \sum \dot{m}_{in} h_{in} \quad (8)$$

$$Q_{out,tank,j} = Q_{loss,top,j} + Q_{loss,bot,j} + Q_{loss,edg,j} + Q_{cond,j} + \sum \dot{m}_{out} h_{out} + Q_{mix,j} \quad (9)$$

where the heat loss from the top, edges, and the bottom of the storage for tank node j are:

$$Q_{loss,top,j} = A_{top,j} U_{top} (T_{tank,j} - T_{env,top}) \quad (10)$$

$$Q_{loss,bot,j} = A_{bot,j} U_{bot} (T_{tank,j} - T_{env,bot}) \quad (11)$$

$$Q_{loss,edg,j} = A_{ed,j} U_{edg} (T_{tank,j} - T_{env,edg}) \quad (12)$$

$A_{top,j}$ represents the tank top surface area for thermal losses (attributed to tank node 1), $A_{bot,j}$ denotes the tank bottom surface area for thermal losses (attributed to tank node N), $A_{edg,j}$ is the tank edge surface area for thermal losses, U_{top} is the storage tank top heat loss coefficient, U_{bot} is the storage tank bottom heat loss coefficient, U_{edg} represents the storage tank edge heat loss coefficient, $T_{tank,j}$ indicates the temperature of individual tank nodes, while, $T_{env,top}$, $T_{env,bot}$, and $T_{env,edg}$ correspond to tank environment temperature for losses through the tank's top, bottom, and edges, respectively.

The nodes in the storage tank can interact thermally via conduction between nodes. The formulation of the conductivity heat transfer from tank node j is:

$$Q_{cond,j} = k_j A_j \frac{T_j - T_{j+1}}{L_j} + k_{j-1} A_{j-1} \frac{T_j - T_{j-1}}{L_{j-1}} \quad (13)$$

where T_j represents the temperature of this node, T_{j+1} is the temperature of the node directly below the current node, T_{j-1} is the temperature of the node directly above the current node; k_j signifies the thermal conductivity of the fluid in node j, k_{j-1} is the thermal conductivity of the fluid in the node directly above the current node; A_j represents the conduction interface area between this node and the one below it, and A_{j-1} is the conduction interface area between this node and the one above it; $L_{cond,j}$ denotes the vertical distance between the centroid of this node and the centroid of the node below, while $L_{cond,j-1}$ represents the vertical distance between the centroid of this node and the centroid of the node above.

$Q_{aux,t}$ is the auxiliary heater input for hot water preparation. At times, the nodes in the storage tank may become thermally unstable (a node has a higher temperature than the node above). If this happens, the model completely mixes any nodes that are unstable at the end of the timestep to avoid problems, $Q_{mix,j}$ is added to the energy balance of the storage tank to account for mixing effects.

3.1.3. Absorption chiller

This component is a single-effect hot-water fired absorption chiller. It is operated using hot water to regenerate the refrigerant in the generator from the refrigerant-absorbent mixture. The component is catalog-based, has its own external file and can predict the chiller's performance within a specified range of input data (Khan et al., 2018). When operating at rated capacity, the design energy input must be provided to the chiller. When the chiller is running at part load, only a fraction of the design energy input is required. With this data, the energy delivered to the chiller by the hot water stream is (Solar Energy Laboratory, 2019):

$$\dot{Q}_{hw} = \frac{\text{Capacity}_{rated}}{\text{COP}_{rated}} f_{DesignEnergyInput} \quad (14)$$

where $\text{Capacity}_{\text{rated}}$ is chiller rated capacity, $\text{COP}_{\text{rated}}$ is the chiller design coefficient of performance, $\text{f}_{\text{DesignEnergyInput}}$ is the fraction of rated capacity required by the cooling machine.

The amount of energy that must be removed from the chilled water stream to bring it from its entering temperature to the setpoint temperature is (Solar Energy Laboratory, 2019):

$$\dot{Q}_{chw} = \dot{m}_{chw} Cp_{chw} \left(T_{chw,in} - T_{chw,set}\right) \quad (15)$$

Where $\dot{\text{m}}_{\text{chw}}$ and Cp_{chw} are the mass flow rate and the specific heat of the chilled water, respectively. The total heat removed from the stream dissipated into the atmosphere in the cooling tower ($\dot{\text{Q}}_{\text{cw}}$) is estimated as (Solar Energy Laboratory, 2019):

$$\dot{Q}_{cw} = \dot{Q}_{hw} + \dot{Q}_{chw} + \dot{Q}_{par} \quad (16)$$

where $\dot{\text{Q}}_{\text{hw}}$ is the energy removed from the hot water stream, $\dot{\text{Q}}_{\text{chw}}$ is the energy removed from the chilled water stream, and $\dot{\text{Q}}_{\text{par}}$ represents the energy consumed by additional components in the system, such as solution pumps, fluid stream pumps, and controls.

It is assumed that the entire energy requirement for auxiliary devices is used whenever the chiller is on, regardless of operating on full or partial load capacity.

3.1.4. Weather data

The hourly weather data of Lund is stored in the TMY-2 (Typical Meteorological Year 2) standard format. Fig. 5 shows the ambient temperature and the global solar radiation in cooling season for Lund, Sweden. The maximum temperature is 28.5 °C, and the horizontal solar radiation reaches above 800 W/m^2 on a summer day.

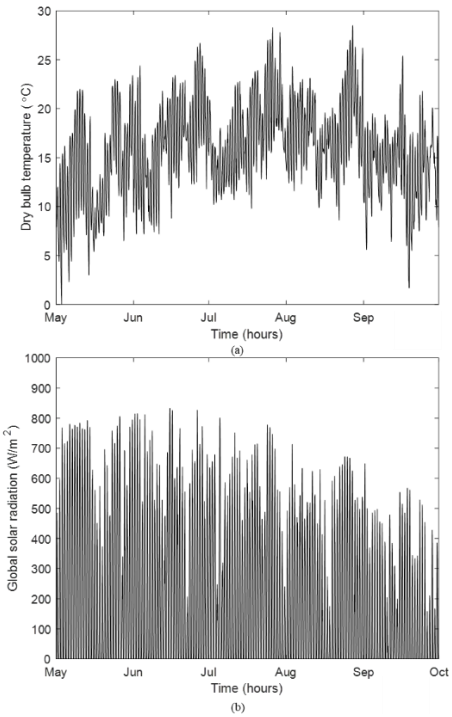

Figure 5. a) ambient temperature and b) global solar radiation on a horizontal plane for Lund in cooling season

3.2. Performance metrics

The evaluation of the performance and effectiveness of an integrated energy system goes beyond solely focusing on efficiency measurements. Therefore, to ensure a holistic approach, additional metrics are analyzed.

Solar fraction is an index used to evaluate the contribution of the solar-driven equipment for cooling and hot water preparation relative to the total energy required to drive the cooling system (Fong, Chow, Lee, Lin, & Chan, 2010).

The solar fraction (SF) is defined as:

$$\text{SF} = \frac{P_{el} + Q_u}{P_{el} + Q_u + Q_{aux,t} + Q_{aux,c}} \quad (17)$$

where P_{el} is the PV/T power output, Q_{u} is the useful energy added by the PV/T to the liquid stream, $\text{Q}_{\text{aux,t}}$ is the auxiliary heater input for hot water preparation, and $\text{Q}_{\text{aux,c}}$ is amount of auxiliary fluid heater input as the energy source for chiller operation.

In addition to the performance metrics, levelized cost of cooling (LCOC) is evaluated as an economic indicator. It represents the price of cooling production and is expressed by (Sajid & Bicer, 2021):

$$\text{LCOC} = \frac{\text{NPC}}{\sum_{i=1}^{25} Q_{cold}} \quad (18)$$

in which Q_{cold} is the amount of heat removal from the building, resulting in a decrease in temperature.

NPC is the net present cost of the system calculated by (Sajid & Bicer, 2021):

$$\mathrm{NPC} = C_I + \sum_{i=1}^{25} \frac{Q_{aux,c} C_{elec} + C_{om}}{(1+r)^i} \quad (19)$$

where r is the discount rate, N is the lifespan of the system, $Q_{aux,c}$ is the auxiliary chiller fluid heater energy consumption, C_{elec} is the unit price of electricity, and C_{om} is the operating and maintenance cost estimated to be 3% of initial investment cost (Sajid & Bicer, 2021).

The investment cost for each of the components is tabulated in Tab. 4. The rest of the key parameters are brought in Tab. 5.

Table 4. Financial specifications of the system

Component	Cost	Reference
Photovoltaic thermal solar collector	$384€/m^2$	(Gu & Zhang, 2021)
Thermal storage tank	$608€/m^3$	(Mortadi & El Fadar, 2022)
Cooling tower	$67.6€/kW$	(Mortadi & El Fadar, 2022)
Single-effect absorption chiller	$300€/kW$	(Saastamoinen & Paiho, 2018)
Inverter	500€	(Reddy Penaka, Kumar Saini, Zhang, & Amo, 2020)
Electric boiler	$78€/kW$	(Zhao, Ge, Sun, Ding, & Yang, 2019)

Table 5. Key input parameters for the simulation.

Parameter	Value	Reference
Electricity price	$0.17€/kWh$	(Gu, Zhang, & Application, 2021)
Discount rate	8%/year	(Gu et al., 2021)
Project lifetime	25 years	(Bellos & Tzivanidis, 2017)

3. Results

The solar system is supposed to be used for cooling as well as hot water preparation. Hence, the scope of simulation is confined from May until the end of September. Using Lund, Sweden as the location of the case study the hot water supply shall be sufficient to satisfy the demands of the establishment. The sanitization and dishwashing, requires higher temperatures for effective cleaning and sterilization so the hot water supply temperature is set to 70°C which is suitable for booster heaters. The tap water temperature is 15 °C. By utilizing the provided information and constructing the model, it becomes possible to generate outcomes that pertain to the performance of the building's energy system throughout the cooling season.

Fig. 6 illustrates the variation of monthly hot water generated during the cooling season. As solar radiation and ambient temperature increase, the rate of energy transfer to the water flowing through the PV/T panels also increases, leading to 313.2 m^3 total produced hot water in June. The monthly produced water cooling is lowest in May and September. For the other months, the amount of water sent toward the chiller is almost constant as the cooling demand rarely has sharp variations in this period.

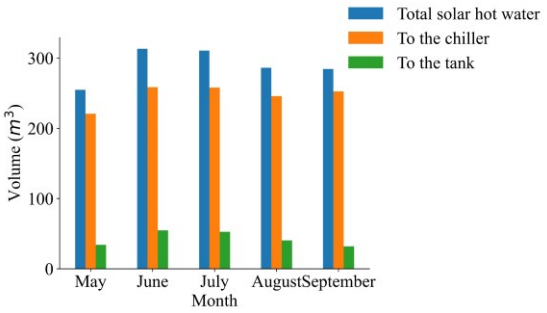

Figure 6. Produced solar hot water volume for each month.

Fig. 7 illustrates the combined heat and electricity produced by the PV/T panels from May to September. It is revealed that the PV/T is more effective at converting solar energy into electricity rather than heat in May and September where there is lower level of solar irradiance. The share of electricity and heat production during the summer months is more balanced which highlights that the PV/T provides a well-rounded energy solution, catering to both electrical and thermal energy needs.

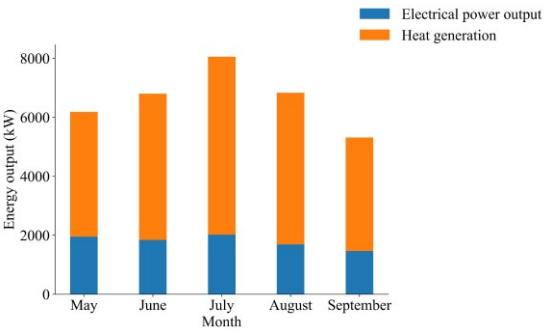

Figure 7. PV/T energy output.

Fig. 8 shows total electricity demand for the operation of the energy system categorized for each component. Among the components, the auxiliary fluid heater has the highest electricity consumption. Due to the lower solar irradiance even in summer months, the thermal energy produced by PVT is generally limited to lower-grade heat, such as hot water preparation. Since the hot water inlet temperature for driving the absorption chiller is 90°C, the additional necessary power required to reach to this setpoint is large relative to other components.

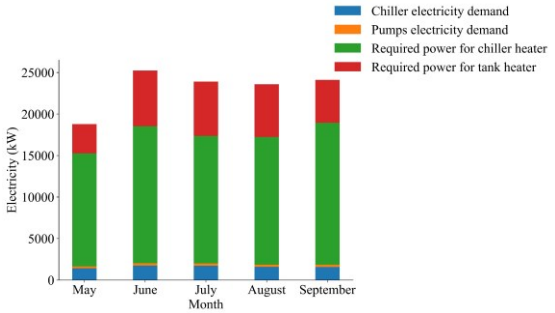

Figure 8. Electricity consumption of each equipment.

A schematic of electricity flows showing possible interactions between the electrical power output from the PV/T and grid electricity to the system is shown in Fig. 9. The total power generated from the PV/T collectors is sufficient to cover the chiller electricity demand. However, the chiller heater relies on grid electricity to meet its power requirement for most of its operation period. It is noticed that only for 16% of the time the reliance on grid is eliminated.

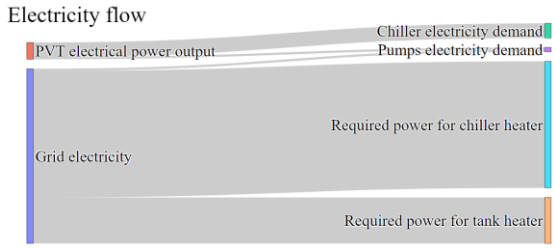

Figure 9. Schematic of electricity flows from PVT and grid to the system.

The cooling generated by the system meets the load requirement, proving the feasibility of the proposed system during the whole simulation period. Besides, it is designed to deliver hot water at a required temperature of 70°C. Fig. 10 shows histograms depicting the distribution of hot water outlet temperatures from the storage tank for each month of the cooling season. The blue bins represent the frequency of hours when the outlet temperature was below the desired setpoint of 70°C. It can be observed that while the average outlet temperature remains close to the setpoint during all months, deviations below the setpoint occur. The percentage of hours below 70°C is higher in the peak summer months of June, July, and August at 49%, 47% and 46% respectively, compared to 23% in May and 34% in September. This occurs as more hot water is diverted to meet the increased cooling demand in summer, causing the tank temperature to drop below the setpoint more often. This is more frequently observed during instances of abrupt changes in water demand, such as in the early morning or after lunch hours. In these scenarios, the recovery time of the auxiliary heater may not be sufficient to keep up with the demand. This can cause the temperature to drop below the setpoint.

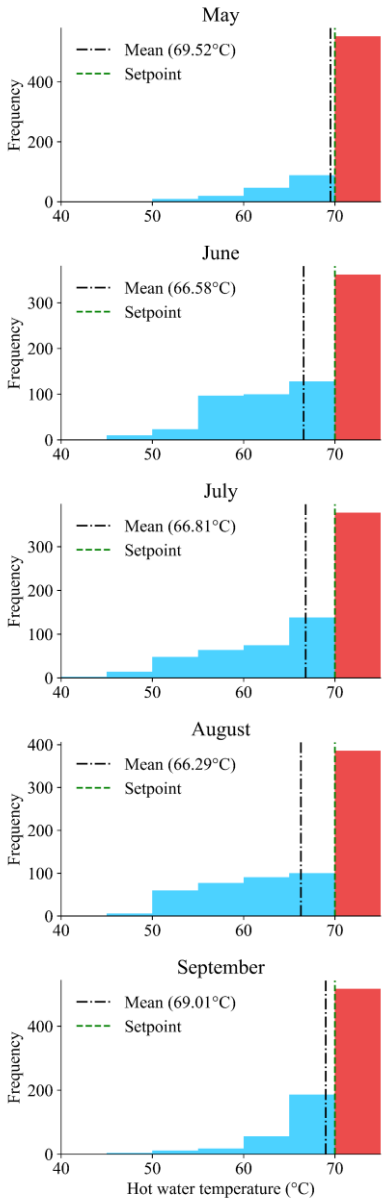

Figure 10. Thermal storage tank outlet temperature violin distribution

Fig. 11 shows the energy performance of the equipment throughout the cooling season. The PVT

has an average thermal efficiency of 28.61% and an electrical efficiency of 6.51%. The single-state absorption chiller average coefficient of performance (COP) is 0.47. From May to August, the solar intensity and ambient temperature increase resulting in higher energy input to the PV/T system and enhanced heat transfer from the PV/T panels and consequently higher thermal efficiency. The system load increases in the summer months. Hence, the absorption chiller may need to operate at higher capacities, which can improve its COP. This is the main reason for the COP drop from August to September.

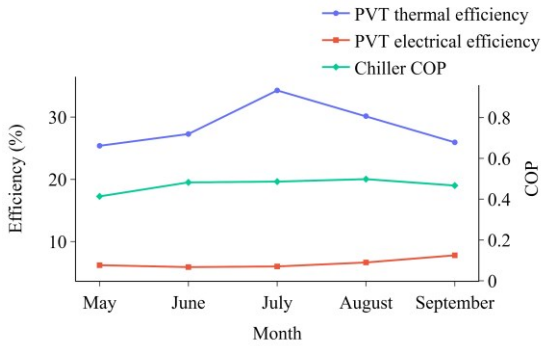

Figure 11. Monthly energy performance of PVT and chiller

Solar-powered integrated energy systems having high solar fractions are more economical (Zhai & Wang, 2009). This metric can be used for comparison between various solar cooling systems. Fig. 12 illustrates the monthly variation of solar fraction throughout the entire cooling season for both the PV/T-based model as well as a model in which the PV/T component is substituted with a solar collector with identical specifications. Another distinction is that the collector-based model is only used for cooling, and hot water supply is discarded. The variation in solar fraction, characterized by higher values in May and September in contrast to the summer months, can be attributed to the reduced cooling demand experienced during these periods for the PV/T-based system. Comparing the annual average values, the solar fraction (SF) for the PV/T-powered system reaches approximately 0.41, which is four times higher than that of the solar collector-based system. Therefore, in solar cooling applications, it is best to integrate them with hot-water supply systems.

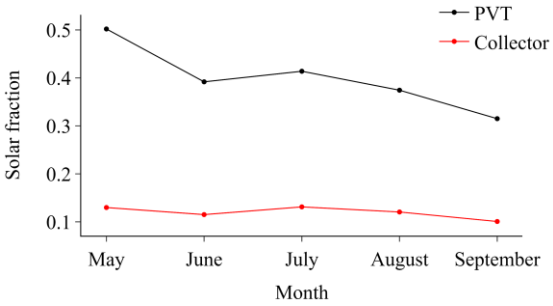

Figure 12. Variation of solar fraction against different months for PV/T and solar collector

To investigate the proposed system from an economic standpoint, the levelized cost of cooling is obtained as 0.164 €/kWh. LCOC provides a standardized approach for comparison among solar thermal cooling systems with absorption chillers. The LCOC values reported by Bellos and Tzivanidis (2017) for solar-thermal absorption chillers for other cities are also depicted in Fig. 13. Generally, locations with higher cooling demand and higher solar radiation attain lower LCOC values. Although the initial investment cost for the proposed PVT-based chiller is higher, the produced cost of cooling is not much higher in comparison with the other cities. It is important to state that the parameter is relatively sensitive to the price of electricity which caused the installation in Madrid with an electricity price of 0.24 €/kWh to be less cost-effective than the present study. Additionally, utilizing PV/T instead of solar thermal collectors offers an added advantage of lowering the levelized cost. This is due to the surplus electricity generated to meet the chiller electricity demand, despite the higher initial investment cost.

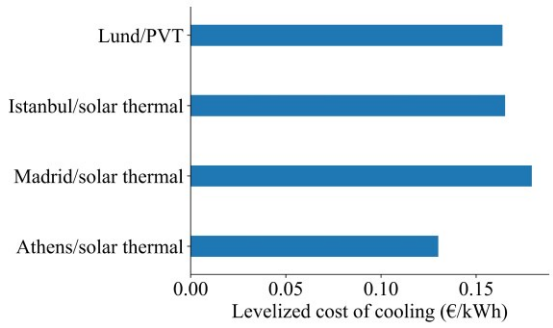

Figure 13. Levelized cost of cooling and installation location for the proposed system and other solar-driven chillers in the literature (Bellos & Tzivanidis, 2017).

4. Summary and Discussions

The cost of cooling is directly linked to the prevailing prices of electricity. Absorption cooling can be increased if there are opportunities to exploit waste heat or renewable heat sources for the process. The feasibility of using a solar-powered absorption chiller for a benchmark model of a full-service

restaurant was assessed. Instead of using the common solar thermal collector, hybrid PV/T collectors were opted for as the hot water production is crucial for a restaurant operation. The system configuration was developed in TRNSYS, and the components were sized based on achieving hot water temperature of 70°C as well as fulfilling the cooling demand. The proposed system met the restaurant's cooling load requirements. It also delivered hot water at the setpoint temperature for many operating hours. However, during peak cooling months the tank outlet temperature deviated below the hot water setpoint more frequently due to abrupt draw increases and limitations in the auxiliary heater recovery time. The surplus electricity generated was found to be sufficient for the chiller operation, provided that all the generated electricity is directed towards it. The PV/T system exhibited an average thermal efficiency of 28.61% and an electrical efficiency of 6.51%. The single-stage absorption chiller achieved an average COP of 0.47. SF and LCOC values confirmed that solar absorption chiller can be a more promising solution in conjunction with PV/T rather than a solar thermal collector in Sweden. This holds particularly true when there is a concurrent demand for electricity and hot water, such as in a restaurant.

Acknowledgment

This research was financially supported by KK-stiftelsen as part of the "SMART- Smart control of district heating networks integrating next generation energy efficient buildings" project.

References

Abdullah, G. F., Saman, W., Whaley, D., & Belusko, M. (2016). Optimization of standalone solar heat fired absorption chiller for typical Australian homes. *Energy Procedia, 91*, 692-701. doi:10.1016/j.egypro.2016.06.232

Behzadi, A., & Arabkoohsar, A. J. E. (2020). Feasibility study of a smart building energy system comprising solar PV/T panels and a heat storage unit. *Energy, 210*, 118528. doi:10.1016/j.energy.2020.118528

Bellos, E., & Tzivanidis, C. (2017). Energetic and financial analysis of solar cooling systems with single effect absorption chiller in various climates. *Applied Thermal Engineering, 126*, 809-821. doi:10.1016/j.applthermaleng.2017.08.005

Borhani, S., Kasaeian, A., Pourmoghadam, P., & Omid, M. (2023). Regional Performance Evaluation of Solar Combined Cooling Heating and Power Systems for Household Demands. *Applied Thermal Engineering, 120666*. doi:10.1016/j.applthermaleng.2023.120666

Boverket. (2019). Boverket´ s Mandatory Provisions and General Recommendations, BBR, BFS 2011: 6 with Amendments up to BFS 2018: 4. In: Boverket Karlskrona, Sweden.

Deru, M., Field, K., Studer, D., Benne, K., Griffith, B., Torcellini, P., . . . Rosenberg, M. (2011). US Department of Energy commercial reference building models of the national building stock.

Fong, K., Chow, T. T., Lee, C. K., Lin, Z., & Chan, L. (2010). Comparative study of different solar cooling systems for buildings in subtropical city. *Solar Energy, 84(2)*, 227-244. doi:10.1016/j.solener.2009.11.002

Fuentes, E., Arce, L., & Salom, J. (2018). A review of domestic hot water consumption profiles for application in systems and buildings energy performance analysis. Renewable and *Sustainable Energy Reviews, 81*, 1530-1547. doi:10.1016/j.rser.2017.05.229

. GenOpt (Version 3.0.0). (2009). http://simulationresearch.lbl.gov/GO: The Regents of the University of California.

Gu, Y., & Zhang, X. (2021). A Solar Photovoltaic/Thermal (PV/T) Concentrator for Building Application in Sweden Using Monte Carlo Method. In X. Zhang (Ed.), Data-driven Analytics for Sustainable Buildings and Cities: From Theory to Application (pp. 141-161). Singapore: Springer Singapore.

Gu, Y., Zhang, X. J. D.-d. A. f. S. B., & Application, C. F. T. t. (2021). A Solar Photovoltaic/Thermal (PV/T) Concentrator for Building Application in Sweden Using Monte Carlo Method. 141-161.

IEA. (2018). The Future of Cooling. Retrieved from Paris: https://www.iea.org/reports/the-future-of-cooling

Khan, M. S. A., Badar, A. W., Talha, T., Khan, M. W., & Butt, F. S. (2018). Configuration based modeling and performance analysis of single effect solar absorption cooling system in TRNSYS. *Energy conversion management, 157*, 351-363. doi:10.1016/j.enconman.2017.12.024

Liu, L., Rohdin, P., & Moshfegh, B. (2015). Evaluating indoor environment of a retrofitted multi-family building with improved energy performance in Sweden. *Energy and Buildings, 102*, 32-44. doi:10.1016/j.enbuild.2015.05.021

Lubis, A., Jeong, J., Saito, K., Giannetti, N., Yabase, H., & Alhamid, M. I. (2016). Solar-assisted single-double-effect absorption chiller for use in Asian tropical climates. *Renewable Energy, 99*, 825-835. doi:10.1016/j.renene.2016.07.055

Mortadi, M., & El Fadar, A. (2022). Performance, economic and environmental assessment of solar cooling systems under various climates. *Energy Conversion and Management, 252*, 114993. doi:10.1016/j.enconman.2021.114993

Murakawa, S., Nishina, D., Takata, H., & Tanaka, A. (2005). An analysis on the loads of hot water consumption in the restaurants. Paper presented at the Proceedings of the 31st W062 International Symposium on Water Supply and Drainage for Buildings, Brussels, Belgium.

Palm, J., & Gustafsson, S. (2018). Barriers to and enablers of district cooling expansion in Sweden. *Journal of Cleaner Production, 172*, 39-45. doi:10.1016/j.jclepro.2017.10.141

Palomba, V., Vasta, S., Freni, A., Pan, Q., Wang, R., & Zhai, X. (2017). Increasing the share of renewables through adsorption solar cooling: A validated case study. *Renewable Energy, 110*, 126-140. doi:10.1016/j.renene.2016.12.016

Reddy Penaka, S., Kumar Saini, P., Zhang, X., & Amo, A. d. (2020). Digital mapping of techno-economic performance of a water-based solar photovoltaic/thermal (PVT) system for buildings over large geographical cities. *Buildings, 10(9),* 148. doi:10.3390/buildings10090148

Saastamoinen, H., & Paiho, S. (2018). Prospects for absorption chillers in Finnish energy systems. *Energy Procedia, 149*, 307-316. doi:10.1016/j.egypro.2018.08.194

Sajid, M. U., & Bicer, Y. (2021). Comparative life cycle cost analysis of various solar energy-based integrated systems for self-sufficient greenhouses. *Sustainable Production and Consumption, 27,* 141-156. doi:10.1016/j.spc.2020.10.025

Solar Energy Laboratory, T. T. E. G., CSTB (Centre Scientifique et Technique du Bâtiment). (2019). In TRNSYS 18 a TRaNsient SYstem Simulation program, Mathematical Reference (Vol. 4, pp. 149-156). United States.

Werner, S. (2017). District heating and cooling in Sweden. *Energy, 126*, 419-429. doi:10.1016/j.energy.2017.03.052

Yue, H., Xu, Z., Chu, S., Cheng, C., Zhang, H., Chen, H., & Ai, D. (2023). Study on the Performance of Photovoltaic/Thermal Collector–Heat Pump–Absorption Chiller Tri-Generation Supply System. *Energies, 16(7)*, 3034. doi:10.3390/en16073034

Zhai, X., & Wang, R. (2009). A review for absorbtion and adsorbtion solar cooling systems in China. *Renewable and Sustainable Energy Reviews, 13(6-7)*, 1523-1531. doi:10.1016/j.rser.2008.09.022

Zhao, S., Ge, Z., Sun, J., Ding, Y., & Yang, Y. (2019). Comparative study of flexibility enhancement technologies for the coal-fired combined heat and power plant. *Energy Conversion and Management, 184,* 15-23. doi:10.1016/j.enconman.2019.01.030